

The influence of droplet concentration on phase change and inertial cavitation thresholds associated with acoustic droplet vaporization

Yanye Yang, Dongxin Yang, Qi Zhang, Xiasheng Guo, Jason L. Raymond, Ronald A. Roy, Dong Zhang, and Juan Tu

Citation: *The Journal of the Acoustical Society of America* **148**, EL375 (2020); doi: 10.1121/10.0002274

View online: <https://doi.org/10.1121/10.0002274>

View Table of Contents: <https://asa.scitation.org/toc/jas/148/4>

Published by the *Acoustical Society of America*

ARTICLES YOU MAY BE INTERESTED IN

Effect of speech volume on respiratory emission of oral bacteria as a potential indicator of pathogen transmissibility risk

The Journal of the Acoustical Society of America **148**, 2322 (2020); <https://doi.org/10.1121/10.0002278>

A Fourier transform formulation for radiation from an un baffled cylinder

The Journal of the Acoustical Society of America **148**, 2311 (2020); <https://doi.org/10.1121/10.0002258>

Nonlinear ultrasound simulation in an axisymmetric coordinate system using a k-space pseudospectral method

The Journal of the Acoustical Society of America **148**, 2288 (2020); <https://doi.org/10.1121/10.0002177>

Observations of upper ocean sound-speed structures in the North Pacific and their effects on long-range acoustic propagation at low and mid-frequencies

The Journal of the Acoustical Society of America **148**, 2040 (2020); <https://doi.org/10.1121/10.0002174>

Context effects on phoneme categorization in children with dyslexia

The Journal of the Acoustical Society of America **148**, 2209 (2020); <https://doi.org/10.1121/10.0002181>

Cathodoluminescence in single and multiwall WS₂ nanotubes: Evidence for quantum confinement and strain effect

Applied Physics Reviews **7**, 041401 (2020); <https://doi.org/10.1063/5.0019913>



The influence of droplet concentration on phase change and inertial cavitation thresholds associated with acoustic droplet vaporization

.....
Yanye Yang,^{1,a)} Dongxin Yang,¹ Qi Zhang,¹ Xiasheng Guo,¹
Jason L. Raymond,^{2,b)} Ronald A. Roy,^{1,a)} Dong Zhang,¹ and Juan Tu¹
¹Key Laboratory of Modern Acoustics (MOE), Department of Physics, Collaborative Innovation Center
of Advanced Microstructure, Nanjing University, Nanjing 210093, China
²Department of Engineering Science, University of Oxford, Oxford, United Kingdom
yanye.yang@smail.nju.edu.cn, dz1622044@smail.nju.edu.cn, qizhang@smail.nju.edu.cn,
guoxs@nju.edu.cn, jason.raymond@eng.ox.ac.uk, ronald.roy@eng.ox.ac.uk, dzhang@nju.edu.cn,
juantu@nju.edu.cn

Abstract: Acoustic droplet vaporization (ADV) is an important process that enables the therapeutic application of acoustically activated droplets, where the nucleation of inertial cavitation (IC) activity must be precisely controlled. This Letter describes threshold pressure measurements for ADV and acoustic emissions consistent with IC activity of lipid-shelled non-superheated perfluoropentane nanodroplets over a range of physiologically relevant concentrations at 1.1-MHz. Under the frequency investigated, results show that the thresholds were relatively independent of concentration for intermediate concentrations (10^5 , 10^6 , and 10^7 droplets/ml), thus indicating an optimal range of droplet concentrations for conducting threshold studies. For the highest concentration, the difference between the threshold for IC and the threshold for ADV was greatly reduced, suggesting that it might prove difficult to induce ADV without concomitant IC in applications that employ higher concentrations. © 2020 Acoustical Society of America. <https://doi.org/10.1121/10.0002274>

[Editor: Charles C. Church]

Pages: EL375–EL381

Received: 30 July 2020 Accepted: 2 October 2020 Published Online: 23 October 2020

1. Introduction

Phase-change nanodroplets exhibit promising potential for use as a next-generation ultrasound (US) contrast agent due to their chemical similarities with microbubbles while offering deeper penetration depth and longer circulation time.¹ Applications of nanodroplets include B-mode US imaging, photoacoustic imaging, phase-contrast imaging, phase aberration correction, sonoporation therapy, blood-brain-barrier opening, embolotherapy and hyperthermia therapy, etc.² Current formulations of droplets generally include a shell (composed of lipids, proteins, polymers, or surfactants) to provide Laplace pressure and a core [usually perfluorocarbons, including octafluoropropane (boiling point -39°C), decafluorobutane (boiling point -2°C), dodecafluoropentane (boiling point 29°C), decafluoropentane (boiling point 55°C), perfluorohexane (boiling point 58°C), etc.] to generate acoustic impedance mismatch after vaporization. In liquid emulsion form, the droplets have a relatively low scattering cross section due to their small size relative to the acoustic wavelength and similar characteristic impedance with the surrounding liquid. Upon liquid-gas phase transition, the resultant gas core (many times that of the original droplet) presents a much larger scattering cross section for ultrasonic waves. Such a process can be achieved acoustically, i.e., through acoustic droplet vaporization (ADV).³ The exact mechanism of ADV is still under investigation with several possibilities proposed, including cavitation, nucleation, droplet deformation, nonlinear propagation, and superharmonic focusing.² After vaporization, under the influence of the US wave, the gaseous bubble would continue to oscillate, either stably or with sufficient energy to collapse inertially due to the momentum of surrounding liquid.^{1,4,5} Inertial cavitation (IC) is of interest due to its ability to induce mechanical and thermal bioeffects (i.e., jetting and enhanced heat deposition),⁶ which can cause potentially dangerous tissue disruption if induced in normal tissues.

Depending on the application concerned, it may be advantageous to either promote or suppress IC activity during ADV. Because the dynamic behavior of microbubbles—including

^{a)}Also at: Department of Engineering Science, University of Oxford, Oxford, United Kingdom.

^{b)}Also at: Oxford-Suzhou Centre for Advanced Research, Suzhou, China.

both stable and inertial cavitation—is influenced by bubble concentration,^{7,8} it is reasonable to presume that droplet concentration may influence the ADV process and particularly the threshold acoustic pressures for phase change and IC behavior. A number of studies have evaluated the phase change or IC threshold of droplets,² with vastly varying thresholds reported that are difficult to compare. We conducted a simultaneous measurement of phase-change echo enhancement and IC noise emissions during ADV over a range of physiologically relevant droplet concentrations. Observations of the threshold acoustic pressures for phase change and IC behavior reported here could provide direct comparison between two thresholds while evaluating the role of concentration in threshold determination.

In order to evaluate the effect of droplet concentration on phase change and IC during the ADV process, IC noise measurements were conducted using a passive sensor positioned confocally with the vaporization-inducing transducer pulse and echogenicity measurements were performed using a linear-array imaging probe positioned downstream of the nucleation site and time-gated such that the same droplet volume used for IC measurements was interrogated. Echogenicity and noise measurements were performed for a wide range of droplet concentrations covering most droplet application concentrations. Phase change and IC thresholds were calculated in accordance with widely recognized methods^{9–11} to provide conformity and comparability, and their dependence on concentration are discussed.

2. Methods

Droplets were synthesized using a thin-film rehydration method^{2,12} combined with US emulsification.¹³ Three phospholipids, namely, DSPC (850365 P, Avanti Polar Lipids, Inc., AL), DSPE-PEG-2000 (880120 P, Avanti Polar Lipids, Inc., AL), and DPPG (840455 P, Avanti Polar Lipids, Inc., AL), were dissolved in mixed solvent of 2:1 v/v chloroform and methanol at a molecular ratio of 36:4:9. The solvent was removed by a rotary evaporator in a 500 ml flask, and the resultant lipid film was resuspended using deionized water (1 mg/ml). Finally, 10 ml of the resuspended lipid solution was sonicated together with 800 μ l perfluoropentane (Strem Chemicals Inc., MA) for a total duration of 20 s in a 50 ml centrifuge tube under ice bath using an ultrasonic processor (VCX 750, Vibra-Cell Processors, Sonic & Materials, Inc., CT) at 30% output setting (20 kHz, 225 W output power approx.). The initial concentration of droplets was determined by first diluting a sample of droplets with pure water by 1:1000, then adding a portion of diluted sample to a hemocytometer and finally examining under a 400 \times magnification microscope. The resultant initial concentration was found to be around 10^{10} droplets/ml. Figure 1(c) shows the size distribution of droplets measured using a particle sizer (sizing range: 0.3 nm–6 μ m) based on dynamic light scattering (Nanobrook 90 Plus Zeta, Brookhaven Instruments, NY). The average

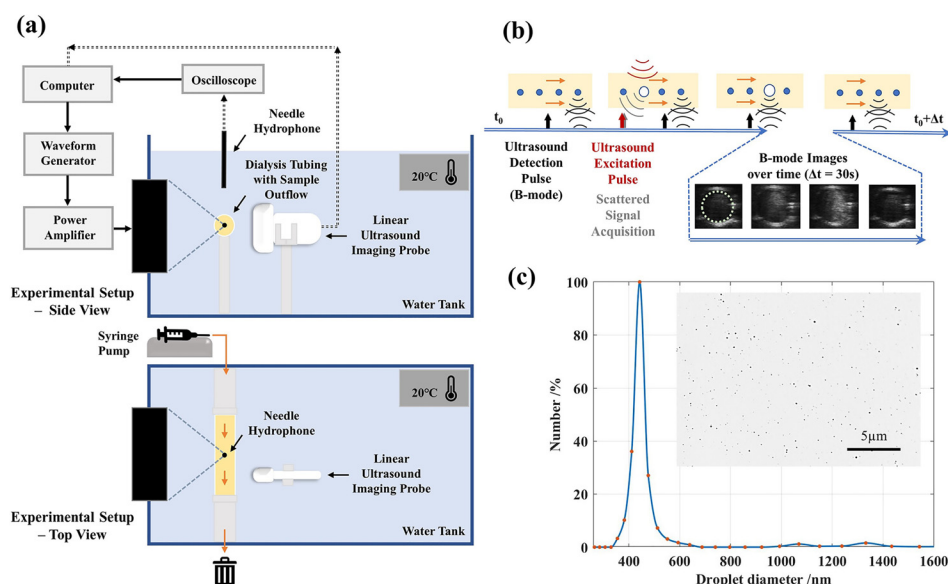


Fig. 1. (Color online) (a) Experimental setup. (b) Flow diagram of data acquisition of a single data point. The B-mode images were stored at 10 Hz frame rate. The dashed circle indicates region of interest (ROI) taken in enhanced echogenicity analysis. The blue double-arrows suggest the time sequence of the illustrated events. The curved lines indicate sound wave, with the black curves standing for B-mode detection pulses and following echo, and the magenta curves standing for ultrasound excitation pulses and the grey the following droplet/bubble acoustic emissions. (c) Size distribution of nanodroplets with the inset showing a microscopic picture of nanodroplets.

hydrodynamic diameter of droplets was calculated to be 462.15 nm under unimodal distribution assumption.

Prior to experiments, droplets were pipette-diluted to designed concentrations (10^4 , 10^5 , 10^6 , 10^7 , and 10^8 droplets/ml) with deionized water whilst the remaining were stored in a refrigerator at 4°C. The diluent was not degassed as it has been previously proven that degassing the carrier liquid showed no statistically significant influence on either ADV threshold or IC threshold.¹⁰

As is shown in Fig. 1(a), a custom-made US transducer (1.1-MHz, 70 mm geometric diameter, -6 dB focal volume = 15.99 mm^3) focused at the center of dialysis tube (MEMBRACEL®, Viskase® Companies, Inc., IL) generated acoustic excitation pulses for droplet vaporization (i.e., the vaporization pulse). Drive signals were generated by a waveform generator (33250 A, Agilent Technologies, CA), passed through a 53-dB power amplifier (2200 L, Electronics and Innovation, Ltd., NY) and an impedance matching box, and sent to the excitation transducer. The focal volume as well as focal peak negative sound pressure of the excitation transducer were determined using a needle hydrophone (s/n 328, Chinese Academy of Sciences, Beijing, China) that was recently calibrated over the frequency range of 1–15 MHz based on reciprocity method. The main lobe of the pressure field near the focus was scanned and the -6 dB focal length and radius were determined to be 9.73 and 0.88 mm, respectively.

In each experiment, 14 tone bursts (10-cycle, 1.1 MHz) were emitted in which the focal peak negative pressure amplitude was increased from 2.95 to 10.13 MPa in increments of 0.55 MPa, with the corresponding peak positive pressure being 3.77 and 39.42 MPa, respectively. The number of cycles was selected such that minimal thermal effect would occur and that the thresholds would fall in a reasonable sound pressure range for the excitation transducer to achieve. The resultant dataset was processed to quantify amplitude-dependent IC noise emission and B-mode enhancement levels. To minimize the likelihood of cavitation in the water outside the tube, the water was degassed and its dissolved oxygen (DO) level was monitored using a DO meter (9010 M, Jenco Inc., CA) to maintain lower than 3 ppm during experiment. Droplet samples were pushed through dialysis tube (6 mm diameter) at a constant volume velocity ($30 \mu\text{l/s}$) using a syringe pump (Legato 270, KD Scientific Inc., MA), and were discarded at the end of tubing. Droplet flow started prior to any measurement and the time between individual pulses was 30 s to ensure bubble-free steady-state conditions prior to every vaporization pulse.

Measurements of the threshold acoustic pressure for phase change are generally achieved through two methods: optical observation of individual droplets or active acoustic detection of gaseous cavities post-vaporization.² While optical observation provides detailed information on the temporal profile of droplet/bubble radial transformation¹⁴ as well as initial nucleation site,¹⁵ its utility is limited by the need for optical transparency, the optical diffraction limitation (limits observation of sub-micron particles), the limited field of view under high magnification (smaller number of observable events), and the complication of a microscope objective in or near the sound beam.¹⁶ Acoustic scattering methods are sensitive to the ensemble average of particles within focal volume (e.g., approximately 155 droplets within the -6 dB focal region given 10^4 droplets/ml in our experiment). The dramatic increase of scattering cross section post-vaporization enables active acoustic detection of phase change, where an interrogation pulse, or two phase-inverted pulses, are sent to interrogate the region of interest and the existence of bubbles can be assessed based on the amplitude and/or frequency content of the scattered signal.^{16,17} One typical application of active acoustic detection is B-mode imaging, a very common form of clinical imaging that enables real-time analysis and is readily accessible to researchers working on biomedical applications of ADV. Thus, B-mode echo enhancement is used here to assess the onset and degree of phase change.

For a quantitative description of phase change behavior, we considered the mean echo enhancement (MEE) of grayscale B-mode images acquired downstream of the excitation transducer focal volume as an indicator of ADV-induced phase change, and the walls of dialysis tube defined the region of interest (ROI). A 7.5-MHz linear-array imaging probe was positioned so that the interrogated region was approximately 4 mm downstream from the focus of the excitation transducer and ADV-formed bubbles started to flow through the imaging volume approximately 1 s after the vaporization pulse. B-mode images were acquired by Terason t3000™ Ultrasound System (Teratech, MA) ($MI < 0.4$), stored at a frame rate of 10 Hz, and processed offline using MATLAB™ (The MathWorks, MA). For each frame acquired, gray scale brightness values within the ROI were summed and normalized by the size of the ROI to quantify the mean echo level (MEL). The background MEL (liquid droplets) was established by averaging a series of B-mode images acquired immediately preceding the vaporization pulse. Thus, the MEE for a particular vaporization pulse amplitude is defined as the background-subtracted MEL averaged over ten repeated measurements.

For IC noise measurements, a needle hydrophone (s/n 328, Chinese Academy of Sciences, Beijing, China) was positioned approximately 4 cm from the center of the acoustic focal region and at 90° to the axial direction of excitation transducer. The position of the hydrophone was adjusted using a small target placed at the focus of the excitation transducer so as to achieve maximum scattered US signal. The hydrophone employed a PVDF sensor with an aperture of 500 μm and a calibrated frequency range of 1–15 MHz. The voltage signal from the hydrophone was acquired by an oscilloscope (54830B, Agilent Technologies, CA) at a sampling rate of 20 MHz, and then transferred to the PC for further analysis.

The onset of IC activity was indicated by the onset of broadband acoustic noise emissions.⁹ We computed the Fast Fourier transform of the noise signal¹⁰ and calculated the root-mean-square (RMS) amplitude of a 1.5 MHz span situated between harmonics of the vaporization pulse (more specifically, three 0.5 MHz windows centered respectively between the first and second, second and third, third and fourth harmonics). The RMS IC noise amplitude was used to quantify the IC dose (ICD). The background ICD signal was established by taking identical measurements with the diluent, water, alone (no droplets) and thus potential cavitation of the diluent was accounted for. The average ICD of the pure water sample obtained over repeated measurements at given acoustic pressure p is denoted $ICD_{w,p}$ with standard deviation $std(ICD_{w,p})$. Signals from samples containing droplets were thus determined to indicate the presence of ADV-related IC activity if the corresponding ICD exceeded $ICD_{w,p} + 9 \times std(ICD_{w,p})$. The criterion for choosing nine standard deviations as a metric for threshold determination has been previously shown to be robust while maintaining enough sensitivity for IC events.¹⁰ Two typical IC threshold-exceeding noise spectra are shown in the inset of Fig. 2(a). For each acoustic pressure amplitude of the vaporization pulse, IC measurements were repeated 10 times and the ratio of the number of IC-occurring measurements to the number of repeated measurements was defined as the probability of IC occurrence at a particular excitation pressure amplitude and concentration of droplets.

For all concentration examined, MEE and the probability of IC occurrence were plotted as functions of vaporization pulse amplitude. Threshold values of phase change and IC were then established by a two-line intersection method¹¹ of sigmoid fitting that took the form of

$$y = \max_{(y)} + \frac{\min_{(y)} - \max_{(y)}}{1 + (x/a)^b}, \quad (1)$$

where $\max_{(y)}$ and $\min_{(y)}$ are the maximum and minimum value within one concentration dataset. The threshold was taken to be the pressure amplitude at the intersection of the two lines fitted, respectively, to the flat and uprising portion of sigmoid.¹¹

3. Results and discussion

Results show that both the MEE and ICD of a known concentration of droplets exhibit a threshold effect, with both MEE and ICD increasing rapidly with increasing vaporization pulse amplitude, albeit at different rates [shown in Fig. 2(a) and 2(b)]. In accordance with previous studies,^{10,17} the IC threshold is generally higher than the B-mode enhancement threshold (phase change threshold) at a particular droplet concentration [see Fig. 2(c)]. This is because, *absent any other cavitation nucleating mechanism*, the free bubbles that undergo inertial cavitation growth and collapse are generated by the vaporization process—it is not possible to have the former without the latter. The threshold for IC, as indicated by the steepness of the response curves, is much sharper than that for droplet vaporization at all concentrations. Both phase change and IC thresholds are shown to shift to lower pressures as concentration increases from 10^4 to 10^8 droplets/ml. For the IC thresholds, the decrease in threshold acoustic pressure is relatively small for low and intermediate concentrations, and drops off significantly at the highest concentration (10^8 droplets/ml). In the case of the MEE, the acoustic pressure decreases with increasing concentration, with a plateau at intermediate concentrations (10^5 , 10^6 , 10^7 droplets/ml). This raises an interesting and important question—why are the IC and phase change thresholds pressures dependent on the concentration of the droplets in the sample?

We consider this question by subdividing the data into three concentration ranges: low (10^4 droplets/ml), intermediate (10^5 , 10^6 , 10^7 droplets/ml), and high (10^8 droplets/ml) concentration. At the low concentration, the spatial distribution of droplets is sparse (inter-droplet distance = 287 μm approximately). If it is assumed that the ICD or MEE signal levels increase with increasing quantities of available cavitation bubbles or vaporization droplets, then a sparse concentration of droplets will invariably yield lower signal levels—possibly too low to detect in the presence of background signal. Thus, higher focal pressure amplitude is required to form a larger volume of threshold-exceeding pressure field that can then vaporize a sufficient number of droplets to yield detectable increases in B-mode enhancement or IC signal level. In such a case, the

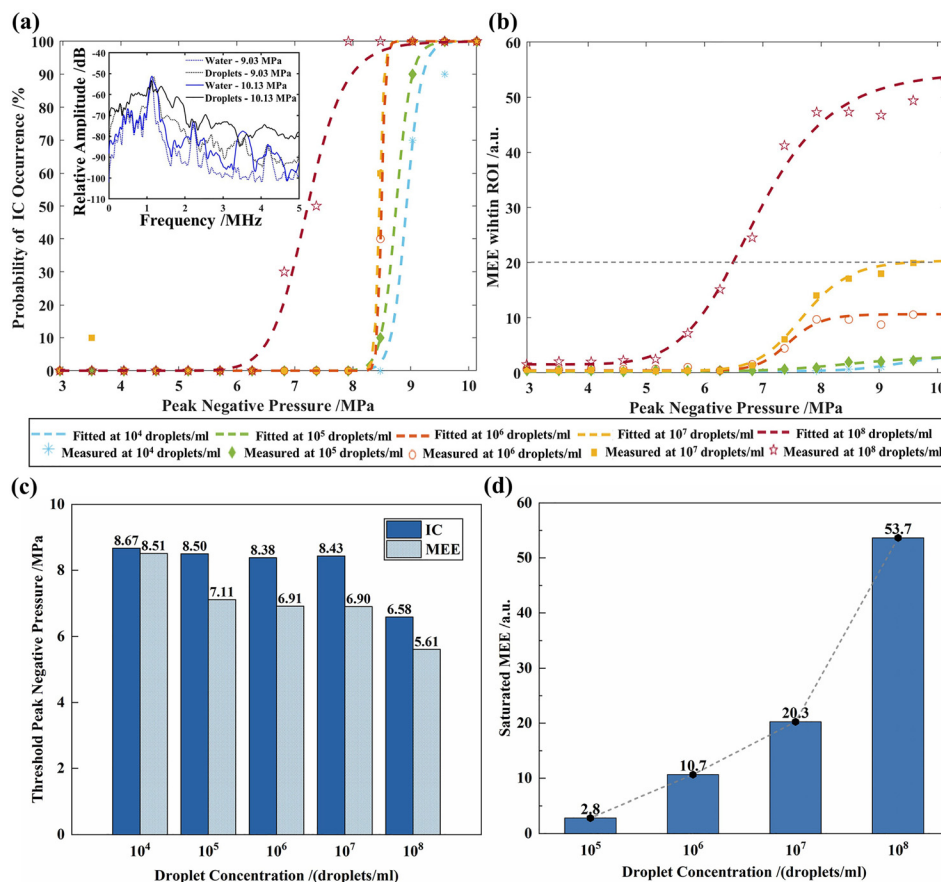


Fig. 2. (Color online) (a) The probability of inertial cavitation (IC) occurrence during ADV under different pressure amplitude at different concentrations. The inset shows two typical spectra of IC threshold-exceeding event acquired at 10^6 droplets/ml with a peak negative pressure of 9.03 (dashed) and 10.13 (solid) MPa. Blue line shows background scattered signals measured with the diluent, water, and the black line shows droplet-scattered signals containing IC at the same pressure amplitude. (b) Mean echo enhancement (MEE) produced by nanodroplets post-ADV under various ADV pressure amplitudes at different concentrations. Grey dashed line indicates the saturated MEE value at 10^7 droplets/ml. (c) IC (dark blue bar) and MEE (light blue bar) threshold acquired from sigmoid fitting. (d) Saturated MEE at various concentrations.

measured threshold is detector dependent. In all instances, regardless of the method used, it is the threshold pressure for detectable activity that is measured, which may be substantially higher than the actual threshold pressure. This seems to be the case for the MEE measurement, for it displays a marked reduction in the measured threshold pressure when the concentration is 10^5 droplets/ml versus 10^4 droplets/ml. The corresponding change in the IC threshold pressure is much smaller.

For intermediate concentrations, the increased number of droplets available for vaporization results in stronger echo/IC signals. Detector sensitivity becomes less of an issue and the thresholds are relatively independent of concentration, as they should be, absent any relevant droplet-droplet interactions. In fact, a similar finding was reported by Zhang and Porter,¹⁸ where they found phase change threshold is independent of droplet volume fractions within the range of 0.15% to 0.40%. The authors are therefore confident that measurements conducted at intermediate concentrations are best estimates of the actual threshold pressures for both vaporization and IC. When droplet concentration further increases to a degree where inter-droplet distance (approximately $13.36 \mu\text{m}$ at 10^8 droplets/ml) become small enough, both the phase change and IC threshold pressures further lower. This cannot be a detector sensitivity issue and must be a reduction in the real threshold pressures. Such finding suggests that at higher concentrations there is indeed a role for droplet-droplet interaction in ADV, a detailed analysis of which is beyond the scope of this Letter. From the point of view of enhancing MEE, it could be as simple as an increased likelihood of bubble coalescence.

It is especially noteworthy that difference between the phase change and IC threshold drops by around 33% (1.39, 1.47, 1.53, and 0.97 MPa at 10^5 , 10^6 , 10^7 , 10^8 droplets/ml, respectively) when the droplet concentration increases to 10^8 droplets/ml. The substantially reduced thresholds and reduced threshold difference at 10^8 droplets/ml suggests that at higher

concentrations it may prove difficult to induce phase change without also generating IC. If one endeavors to enhance a diagnostic objective (better US images through ADV) without inducing a concomitant cavitation bioeffect, droplet concentrations greater than about 10^8 droplets/ml are to be avoided.

Another interesting effect is seen in Fig. 2(b), where one observes that the MEE plateaus for higher amplitude vaporization pulses. Presumably, this is because one reached a vaporization pulse amplitude for which all available droplets are vaporized and increasing the vaporization pulse amplitude has little added effect. While the value at saturation increased with nearly equal differences from 10^5 , 10^6 , to 10^7 droplets/ml, it increased dramatically at 10^8 droplets/ml [as is shown in Fig. 2(d)]. This could be explained by hydrodynamic effects, where bubbles are made to agglomerate into a higher density cloud, or by bubble coalescence, which is more likely to occur at higher concentrations.¹⁹ This effect may even happen in the presence of DSPE-PEG-2000, as it was shown that droplets can expand multiple times after vaporization.²⁰ The scattering cross section of sub-resonance size bubbles is proportional to r^6 ,²¹ where r is the radius. For such bubbles, any increase in size resulting from coalescence will invariably yield a net increase in MEE, even if the total volume of free gas in the flow remains the same.

4. Conclusions

This Letter describes threshold acoustic pressure measurements for two important phenomena—droplet vaporization and IC of the resulting bubbles—associated with the acoustically induced vaporization of non-superheated lipid-coated nanodroplets over a wide range of concentrations. Results show that under 1.1-MHz vaporization pulses, extremely high or low concentrations may alter the measured phase change and IC threshold value, either due to detector sensitivity limitations at low concentrations (10^4 droplets/ml) elevating the *perceived* threshold, or droplet-droplet interaction at high concentrations (10^8 droplets/ml) lowering the *actual* threshold. While ADV phase change occurred at a lower excitation pressure amplitude than IC at all concentrations, the difference between the two thresholds became smaller at 10^8 droplets/ml. There are important safety implications in this result, for it suggests that at higher concentrations, it may prove difficult to induce ADV for enhancement of diagnostic US without also inducing IC and associated deleterious bioeffects.

Considering the fact that the study and characterization of droplets is usually performed using intermediate droplet concentrations (10^5 – 10^7 droplets/ml), whilst *in vivo* applications generally employ higher concentration, the authors hope that the findings of this study will provide researchers with guidance on the selection of concentration and excitation sound pressure best suited to specific applications.

Acknowledgment

This work was supported by the National Key Research and Development Program of China (Grant No. 2018YFC0115901), the National Natural Science Foundation of China (Grant Nos. 11911530173, 11934009, 11874216, 11774168, 11774166, and 81627802), and the UK-China Joint Research and Innovation Partnership Fund (Newton Fund) Ph.D. Placement Program (Grant No. 201806190303). Travel funds were provided in part by the NSFC-Royal Society International Exchanges Cost Share award (No. IEC\NSFC\181326).

References and links

- ¹H. Lea-Banks, M. A. O'Reilly, and K. Hynynen, "Ultrasound-responsive droplets for therapy: A review," *J. Control. Rel.* **293**, 144–154 (2019).
- ²M. Aliabouzar, K. N. Kumar, and K. Sarkar, "Acoustic vaporization threshold of lipid-coated perfluoropentane droplets," *J. Acoust. Soc. Am.* **143**, 2001–2012 (2018).
- ³J. D. Rojas and P. A. Dayton, "Optimizing acoustic activation of phase change contrast agents with the activation pressure matching method: A review," *IEEE Trans. Ultrason. Ferroelectr. Freq. Control* **64**, 264–272 (2017).
- ⁴P. S. Sheeran and P. A. Dayton, "Improving the performance of phase-change perfluorocarbon droplets for medical ultrasonography: Current progress, challenges, and prospects," *Scientifica* **2014**, 579684.
- ⁵Z. Z. Wong, O. D. Kripfgans, A. Qamar, J. B. Fowlkes, and J. L. Bull, "Bubble evolution in acoustic droplet vaporization at physiological temperature via ultra-high speed imaging," *Soft Matter* **7**(8), 4009–4016 (2011).
- ⁶C. C. Coussios and R. A. Roy, "Applications of acoustics and cavitation to noninvasive therapy and drug delivery," *Annu. Rev. Fluid Mech.* **40**, 395–420 (2008).
- ⁷Y. Lin, L. Lin, M. Cheng, L. Jin, L. Du, T. Han, L. Xu, A. C. H. Yu, and P. Qin, "Effect of acoustic parameters on the cavitation behavior of SonoVue microbubbles induced by pulsed ultrasound," *Ultrasonics Sonochem.* **35**, 176–184 (2017).
- ⁸J. Tu, T. J. Matula, A. A. Brayman, and L. A. Crum, "Inertial cavitation dose produced in ex vivo rabbit ear arteries with Optison (R) by 1-MHz pulsed ultrasound," *Ultrasound Med. Biol.* **32**, 281–288 (2006).
- ⁹Y. Gu, C. Chen, J. Tu, X. Guo, H. Wu, and D. Zhang, "Harmonic responses and cavitation activity of encapsulated microbubbles coupled with magnetic nanoparticles," *Ultrasonics Sonochem.* **29**, 309–316 (2016).

- ¹⁰M. L. Fabiilli, K. J. Haworth, N. H. Fakhri, O. D. Kripfgans, P. L. Carson, and J. B. Fowlkes, "The role of inertial cavitation in acoustic droplet vaporization," *IEEE Trans. Ultrason. Ferroelectr. Freq. Control* **56**, 1006–1017 (2009).
- ¹¹O. D. Kripfgans, J. B. Fowlkes, D. L. Miller, O. P. Eldevik, and P. L. Carson, "Acoustic droplet vaporization for therapeutic and diagnostic applications," *Ultrasound Med. Biol.* **26**, 1177–1189 (2000).
- ¹²P. S. Sheeran, S. Luois, P. A. Dayton, and T. O. Matsunaga, "Formulation and acoustic studies of a new phase-shift agent for diagnostic and therapeutic ultrasound," *Langmuir* **27**, 10412–10420 (2011).
- ¹³Y. Zhou, "Application of acoustic droplet vaporization in ultrasound therapy," *J. Therapeutic Ultrasound* **3**, 20 (2015).
- ¹⁴P. S. Sheeran, T. O. Matsunaga, and P. A. Dayton, "Phase change events of volatile liquid perfluorocarbon contrast agents produce unique acoustic signatures," *Phys. Med. Biol.* **59**, 379–401 (2014).
- ¹⁵D. S. Li, O. D. Kripfgans, M. L. Fabiilli, J. B. Fowlkes, and J. L. Bull, "Initial nucleation site formation due to acoustic droplet vaporization," *Appl. Phys. Lett.* **104**, 063703 (2014).
- ¹⁶N. Reznik, R. Williams, and P. N. Burns, "Investigation of vaporized submicron perfluorocarbon droplets as an ultrasound contrast agent," *Ultrasound Med. Biol.* **37**(8), 1271–1279 (2011).
- ¹⁷K. C. Schad and K. Hynynen, "In vitro characterization of perfluorocarbon droplets for focused ultrasound therapy," *Phys. Med. Biol.* **55**, 4933–4947 (2010).
- ¹⁸P. Zhang and T. Porter, "An in vitro study of a phase-shift nanoemulsion: A potential nucleation agent for bubble-enhanced HIFU tumor ablation," *Ultrasound Med. Biol.* **36**(11), 1856–1866 (2010).
- ¹⁹K. J. Haworth and O. D. Kripfgans, "Initial growth and coalescence of acoustically vaporized perfluorocarbon microdroplets," in *2008 IEEE Ultrasonics Symposium*, IEEE (2008).
- ²⁰P. S. Sheeran, V. P. Wong, S. Luois, R. J. McFarland, W. D. Ross, S. Feingold, T. O. Matsunaga, and P. A. Dayton, "Decafluorobutane as a phase-change contrast agent for low-energy extravascular ultrasonic imaging," *Ultrasound Med. Biol.* **37**(9), 1518–1530 (2011).
- ²¹E. P. Stride and C. C. Coussios, "Cavitation and contrast: The use of bubbles in ultrasound imaging and therapy," *Proc. Inst. Mech. Eng. Part H: J. Eng. Med.* **224**, 171–191 (2010).